High-Performance Capacitive Deionization Disinfection of Water with Graphene Oxide-*graft*-Quaternized Chitosan Nanohybrid Electrode Coating

Yilei Wang,[†,‡,△] Ahmed G. El-Deen,[†,‡,△] Peng Li,[*,†,‡,§,△] Bernice H.L. Oh,[†,‡,△] Zanru Guo,[†,‡] Mya Mya Khin,[†,‡] Yogesh S. Vikhe,[†] Jing Wang,[†] Rebecca G. Hu,[∥] Remko M. Boom,[⊥] Kimberly A. Kline,[#,¶] David L. Becker,[∥] Hongwei Duan,[*,†] and Mary B. Chan-Park[*,†,‡]

[†]School of Chemical and Biomedical Engineering, Nanyang Technological University, Singapore 637459, [‡]Centre for Antimicrobial Bioengineering, Nanyang Technological University, Singapore 637459, [§]Centre for Biomedical Engineering and Regenerative Medicine, Frontier Institute of Science and Technology, Xi'an Jiaotong University, Xi'an 710049, China, [∥]Lee Kong Chian School of Medicine, Nanyang Technological University, Singapore 308232, [⊥]Food Process Engineering Laboratory, Agrotechnology and Food Sciences Group, Wageningen University, Wageningen 6708 WG, The Netherlands, [#]Singapore Centre on Environmental Life Sciences Engineering, Nanyang Technological University, Singapore 637551, and [¶]School of Biological Sciences, Nanyang Technological University, Singapore 637551. [△]Y.W., A.G.E.-D., P.L., and B.H.L.O. contributed equally.

ABSTRACT Water disinfection materials should ideally be broad-spectrum-active, nonleachable, and noncontaminating to the liquid needing sterilization. Herein, we demonstrate a high-performance capacitive deionization disinfection (CDID) electrode made by coating an activated carbon (AC) electrode with cationic nanohybrids of graphene oxide-*graft*-quaternized chitosan (GO-QC). Our GO-QC/AC CDID electrode can achieve at least 99.9999% killing (*i.e.*, 6 log reduction) of *Escherichia coli* in water flowing continuously through the CDID cell. Without the GO-QC coating, the AC electrode alone cannot kill the bacteria and adsorbs a much smaller fraction (<82.8 ± 1.8%) of *E. coli* from the same biocontaminated water. Our CDID process consists of alternating cycles of water disinfection followed by electrode regeneration, each a few minutes duration, so that this water disinfection process can be continuous and it only needs a small electrode voltage (2 V). With a typical brackish water biocontamination (with 10^4 CFU mL^{-1} bacteria), the GO-QC/AC electrodes can kill 99.99% of the *E. coli* in water for 5 h. The disinfecting GO-QC is securely attached on the AC electrode surface, so that it is noncontaminating to water, unlike many other chemicals used today. The GO-QC nanohybrids have excellent intrinsic antimicrobial properties in suspension form. Further, the GO component contributes toward the needed surface conductivity of the CDID electrode. This CDID process offers an economical method toward ultrafast, contaminant-free, and continuous killing of bacteria in biocontaminated water. The proposed strategy introduces a green *in situ* disinfectant approach for water purification.

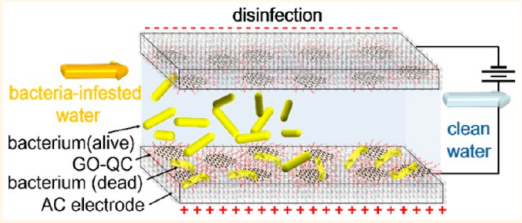

KEYWORDS: water disinfection · capacitive deionization · cationic · contact-active · antimicrobial · graphene oxide · quaternary chitosan

A facile noncontaminating water disinfection approach is in worldwide demand, and approximately, 750 million people around the world have no or little access to clean water.[1,2] The 2015 Global Risk Report published by the World Economic Forum (WEF) has recently identified that clean water scarcity is the most serious risk facing the world at large.[3] Many current water disinfectant agents effectively annihilate pathogenic microorganisms in drinking water but are generally toxic themselves or may produce side products that are harmful to human health.[4] For example, strong oxidizing agents such as hypochlorite and ozone commonly used in water disinfection produce harmful byproducts which can be carcinogenic, mutagenic, or teratogenic. Other disinfectants such as chlorine, phenol, peroxides, and silver nanoparticles, which generally work by solvation into the biocontaminated water, are toxic to

* Address correspondence to lipeng08@xjtu.edu.cn, hduan@ntu.edu.sg, mbechan@ntu.edu.sg.

Received for review June 20, 2015 and accepted September 21, 2015.

Published online September 21, 2015
10.1021/acsnano.5b03763

humans.[5−8] Further, multi-drug-resistant bacteria that are difficult to treat are on the rise.[9,10] At present, there is great demand for new disinfection techniques which meet higher safety standards but are still effective toward a broad spectrum of pathogenic microbes. However, it has been challenging to develop novel agents which effectively kill a broad spectrum of bacteria with zero/negligible contamination to the water needing disinfection.

A new class of antimicrobial agents based on a contact-active mechanism that kills microbes on contact by physical disruption of the anionic microbe cytoplasmic membrane has attracted widespread interest;[11−13] these molecules which are typically cationic polymers or peptides are thought to be less susceptible to microbe resistance than are conventional antibiotics.[14,15] However, many contact-active antimicrobial agents are also toxic as charge-based killing is generally indiscriminately effective against both bacterial and mammalian cells. We have previously discovered that cationic polysaccharides have generally lower toxicity and similar effectiveness compared to non-saccharide-based antimicrobial peptides and polymers.[16,17] Nevertheless, for water disinfection, it would be ideal to avoid adding disinfecting chemicals to the water to be treated. Ideally, the disinfection process would be continuous rather than batch, membrane-free, and consume little energy. It is challenging to find such a process.

Contact-active cationic particles made by tethering cationic polymers or peptides onto particle surfaces are a new type of antimicrobial agent.[18,19] The particulate form of a cationic antimicrobial agent may be more effective than the solution form as the charges are concentrated. Further, the particle may impart unique functional properties to the resulting composite. Graphene oxide (GO), a single-atom-thick two-dimensional (2D) material with micron-scale lateral dimension, appears to be an attractive carrier substrate due to its large specific surface area. For the GO−cationic polymer hybrid, the polymer also serves a supplementary role as a dispersion agent to individually disperse the nanohybrid particles in water to maximally expose the tethered charges. With the large GO surface area, we may easily increase the grafting density to increase the killing efficacy and stability of the nanohybrid. Previous antimicrobial graphene/GO-based antimicrobial agents are composite materials which release the biocides (*e.g.*, Ag ions, phosphonium salts, *etc.*) into solution.[20−26] Recently, a GO−polylysine nanohybrid was made by physically adsorbing the cationic polylysine onto GO, but the polylysine can be desorbed into the aqueous environment.[27] The possible release of the active antimicrobial agents from GO makes the previous GO-based composites not ideally suited for disinfecting water, and they may pose an environmental hazard with long-term use.[28] Further, the nanoscale thickness of the GO-based nanohybrid makes its suspension in water relatively stable and its recovery from water highly challenging. Also, it is not practical to recover GO-based composites after dispersion into large water volumes by filtration or centrifugation.

On the other hand, capacitive deionization (CDI) has shown great promise for the deionization of ions from brackish water.[29−31] It is a continuous-flow process that employs alternating cycles of ion electrosorption to remove ions from the aqueous solution followed by ion desorption from the electrodes to regenerate the latter. The electrodes are usually carbon-based materials, and a low electrical potential (usually 2 V) is typically applied during the ion capture. The CDI deionization process is attractive because of its low power requirement, high regeneration potential, use of nonhazardous chemical in the pre/post-treatment stages, and it is membrane-free. CDI is already applied to water desalination by removing ions from aqueous solutions flowing past two oppositely charged electrodes.[32,33] Bacteria also have negatively charged surfaces, but they are much larger than the salts typically removed by a normal CDI process. There is a recent report on the application of CDI for water disinfection using commercially activated carbon cloth electrodes but the bacteria were not killed but only adsorbed on the electrodes, and the reported degree of removal (not killing) was only $82.8 \pm 1.8\%$, that is, less than 1 log reduction; the bacteria loading investigated was also moderate (10^4 CFU mL^{-1}).[34]

We report herein a novel contact-active graphene oxide-*graft*-quaternized chitosan (GO-QC)-coated activated carbon (AC) electrode for ultrahigh disinfection performance *via* a capacitive deionization disinfection (CDID) process (Figure 1). First, we synthesized GO-QC nanohybrid particles by covalently grafting cationic QC, specifically dimethyldecylammonium chitosan (DMDC), onto GO (Figure 1a). The GO-*graft*-cationic polysaccharide has both good antimicrobial and good hemolytic properties (Table 1). The GO-QC in water shows broad spectrum antimicrobial activity against three clinically significant pathogens and minimum bactericidal concentrations (MBCs of 5−30 μg mL^{-1}) even lower than those of the QC polymer alone (16−60 μg mL^{-1}) or GO (>5000 μg mL^{-1}) alone. Field emission scanning electron microscopy (FESEM) and adenosine triphosphate (ATP) leakage tests were also carried out in order to investigate the antimicrobial mechanism of the GO-QC nanohybrid.

Second, by coating a thin GO-QC particulate layer on the AC electrodes, our CDID process displays an ultrafast, contact-active, efficacious microbicidal effect. Under test conditions of ultrahigh *E. coli* loading (10^6 CFU mL^{-1}) in flowing water, our CDID can achieve more than 99.9999% (*i.e.*, 6 log reduction) bacteria killing; the AC electrodes without the disinfecting

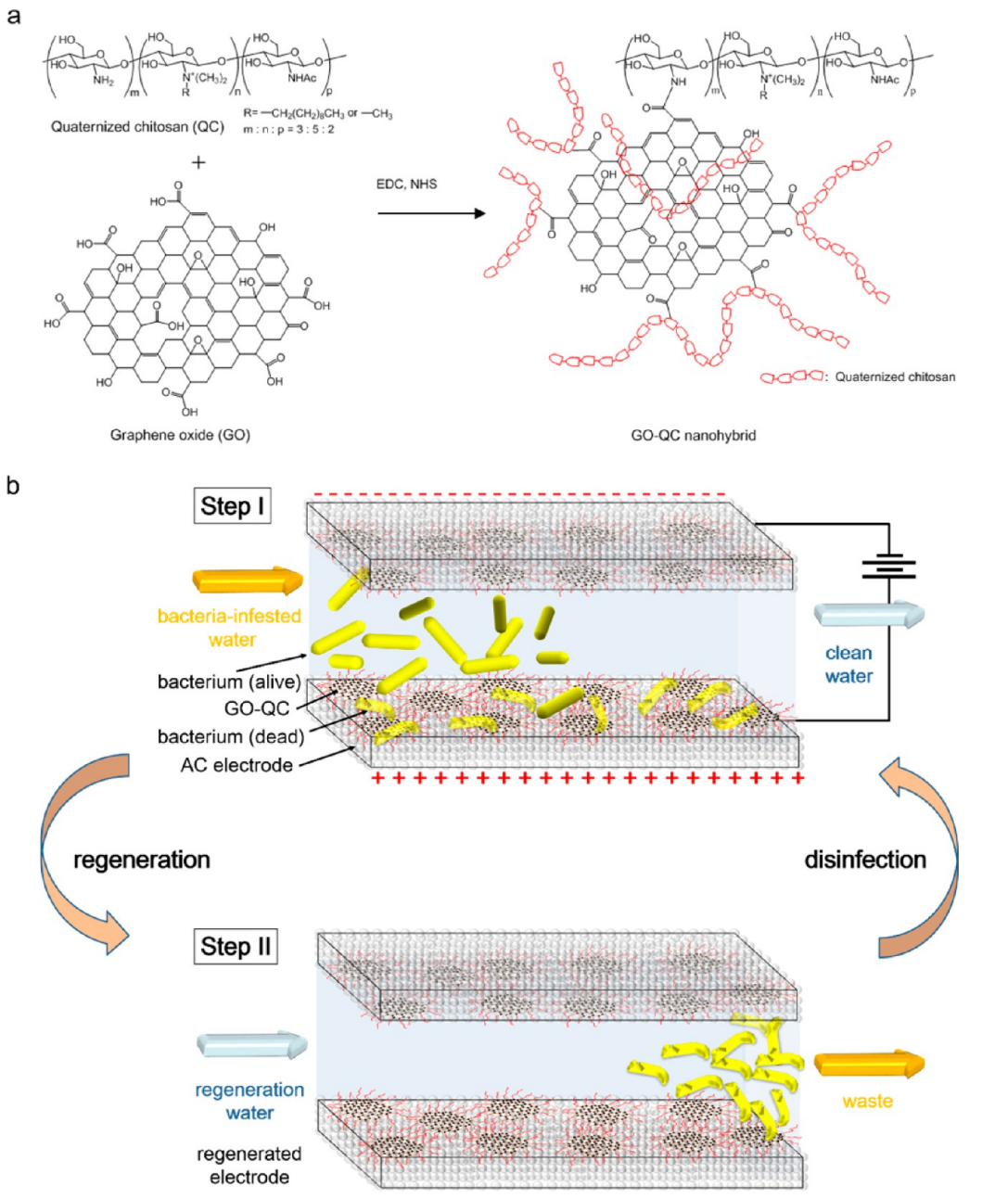

Figure 1. (a) Chemical structure of quaternized chitosan and synthesis schematic of the GO-QC nanohybrid by an amine coupling reaction in the presence of 1-ethyl-3-(3-(dimethylamino)propyl)carbodiimide (EDC) and *N*-hydroxysuccinimide (NHS). (b) Schematic of capacitive deionization disinfection and regeneration of the GO-QC/AC electrode for the continuous disruption of the anionic microbial envelopes, which leads to microbe cell death.

GO-QC layer cannot kill bacteria but can remove some of them from water but with much lower efficiency, that is, less than 1 log reduction. Noteworthy, the AC electrode coated with QC alone in a continuous film form is nonconductive and cannot be used for the CDID process. We also showed that the GO-QC/AC electrode has very good disinfection capacity for bio-contaminated water with different NaCl concentrations (100 and 200 mg L^{-1}) in the range typically found in brackish water. After some saturation with bacteria, the GO-QC/AC electrode can be desorbed of killed bacteria by flushing the electrodes with pure water under 0 V cell potential between the disinfection cycles (Figure 1b). The CDID cell can be run for at least 10 consecutive cycles of bacteria killing alternated by bacteria desorption for the ultrahigh bacteria loading. With a lower (10^4 CFU mL^{-1}) but still relevant bacteria loading to brackish water, the GO-QC/AC electrode can continuously achieve 99.99% bacteria killing for at least 5 h. The GO-QC-coated layer shows some electrical surface conductivity with finite measurable resistivity of 4.83 $\pm$ 0.78 MΩ sq^{-1}, in contrast to the insulating QC polymer alone (with infinity resistivity), so that the GO-QC-coated AC electrode construct is conductive

TABLE 1. Minimum Bactericidal Concentrations and Hemolytic Activities

		A	B			C
			MBC (μg mL^{-1})/selectivity[a]			
no.	materials	GO/QC ratio determined by TGA	*E. coli* (Gram −)	*S. aureus* (Gram +)	*C. albicans* (fungi)	HC_{50} (μg mL^{-1})
1	QC (DMDC)		60/250	30/500	16/938	15000
2	GO		>5000/<0.4	>5000/<0.4	>5000/<0.4	1250
3a	GO-QC (1:1)[b]	1:0.54	310/8	160/16	160/16	2500
3b	GO-QC (1:2.5)	1:1.04	80/63	40/125	20/250	5000
3c	GO-QC (1:5)	1:2.07	30/333	10/1000	5/2000	10000
3d	GO-QC (1:10)	1:2.20	30/333	10/1000	5/2000	10000
4	nCS		>2500	>2500	>2500	>3850

[a] Selectivity = HC_{50}/MBC. [b] Design ratios.

enough to be used as an electrode. Also, the large surface/volume ratio of GO facilitates its fixing on the electrode with a small amount of binder, which prevents contamination of the water flowing through the CDID cell. We show that the GO-QC/AC electrode can be used to realize an energy-efficient and continuous process to disinfect biocontaminated water with no observable leaching into or contamination of the water.

RESULTS AND DISCUSSION

Quaternized chitosan (QC, specifically dimethyldecylammonium chitosan) was synthesized as previously described.[16] Briefly, chitosan (82% deacetylated) was N-alkylated with decanal and then methylated with methyl iodide (Supporting Information Figure S1).[24] The synthesized QC has a quaternization degree of 56% and molecular weight of 38 kDa (Supporting Information Figure S2). Separately, GO nanoflakes were chemically exfoliated from natural graphite powder following Hummers method,[35,36] which is known to introduce abundant oxidized functional groups, including carboxyl groups.[37] The GO nanoflakes have an average thickness of about 1 nm and an average diameter of 746 ± 308 nm (Figure 2a,b and Supporting Information Figure S3a,b). Then a series of GO-QC derivatives were synthesized with designed weight ratios of GO to QC varying from 1:1 to 1:10 (w/w) (Table 1) *via* the reaction of −COOH on GO and the residual $-NH_2$ on QC (Figure 1a).

The AC electrode was fabricated in a manner similar to that for a normal CDI electrode according to previous reports (see Materials and Methods).[38] To prepare the disinfecting GO-QC layer, a mixture of GO-QC and polyvinylidene fluoride (PVDF) in the ratio of 9:1 (w/w) was dissolved in *N*,*N*-dimethylformamide (DMF) solvent and mixed into a uniform slurry. The GO-QC/PVDF slurry was cast on top of an AC electrode (10 cm × 10 cm). After the solvent was dry, the electrode was immersed into DI water to remove the bubbles inside the coating layer and was then ready for use.

Figure 1b shows the architecture and application of our novel GO-QC/AC electrode. Two QC-QC/AC electrodes each with a disinfecting surface coating of the GO-QC nanohybrid were placed parallel to each other and assembled into a CDID cell. Bacteria-contaminated water was pumped through the space between the two GO-QC/AC electrodes. With the application of a small potential (2 V), the bacteria in the flowing water were electrically attracted onto the positive electrode due to the negative charges on their cell envelope and then killed by the GO-QC nanohybrid coating when in physical contact. The electrodes can be regenerated and cleared of bacteria by switching off the voltage and passing non-biocontaminated water through the cell for rinsing.

Figure 2a and Supporting Information Figure S3 show that both GO and GO-QC nanohybrids are individual nanoflakes. Atomic force microscopy (AFM) imaging of the GO-QC (1:5) (Figure 2b) indicates that the average thickness is increased to about 2 nm, while the average diameter of the GO-QC (1:5) nanohybrid is not much changed (573 ± 160 nm) by the QC grafting. Figure 2c displays Fourier transform infrared (FTIR) spectra of pristine GO, QC, and a typical GO-QC (1:5). The peak at 1535 cm^{-1} in the GO-QC spectrum, which is absent in the GO spectrum, corresponds to the newly formed −NHCO− bond between GO and QC, corroborating that QC molecules have been grafted onto the GO through an amide linkage. In the spectrum of QC, there is also a weak peak at 1535 cm^{-1}, which is due to the incomplete deacetylation of chitosan. In addition, X-ray photoelectron spectroscopy (XPS) analysis further confirmed the covalent bonding of QC onto GO (Supporting Information Figure S4).

Thermogravimetric analysis (TGA) (Figure 2d) of GO indicates that 4% of its weight is lost below 100 °C, which is attributable to evaporation of adsorbed water.[39] The major weight loss of GO was observed between 165 and 215 °C, which is likely caused by thermal degradation of oxygen-containing groups present.[40] In contrast, QC has less than 2% weight loss

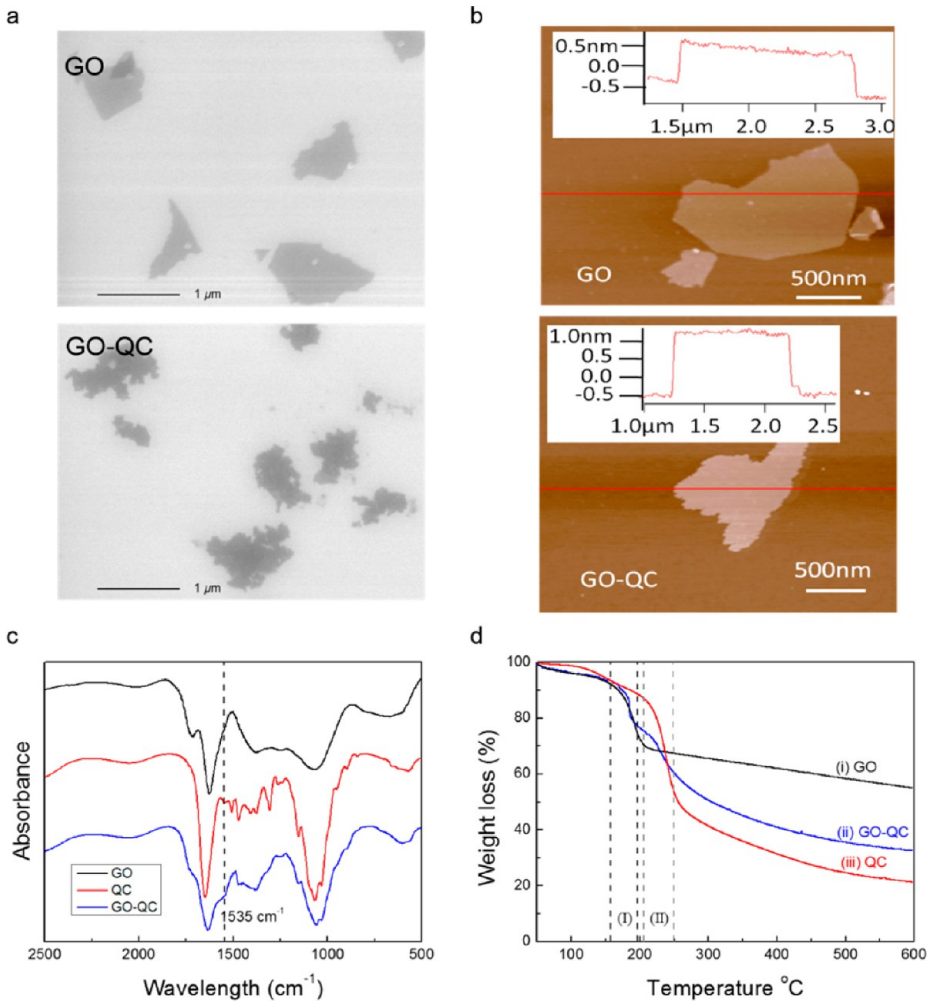

Figure 2. (a) FESEM image of GO and GO-QC (1:5). (b) AFM image of GO and GO-QC (1:5) with the thickness determination. (c) FTIR spectra of GO, QC, and GO-QC (1:5). (d) TGA curves of (i) GO, (ii) GO-QC (1:5), and (iii) QC at a heating rate of 10 °C/min under nitrogen protection.

below 100 °C but 35% weight loss between 210 and 250 °C, which is due to the cleavage of substituent groups and decomposition of glucopyranose rings.[41] The weight loss curve of GO-QC has two stages which can be attributed, respectively, to the major losses of GO (165−195 °C, Stage I) and QC (210−250 °C, Stage II). From the weight losses in these two main regimes, the actual weight ratios of GO to QC can be inferred, and these values differ from the GO/QC design ratios (Table 1). For the design GO/QC reactant weight ratios of 1:1 to 1:5, the measured GO/QC ratios were, respectively, 1:0.54 to 1:2.07, indicating that around 50% of design QC molecules were successfully grafted onto GO nanoflakes. However, for the design GO/QC weight ratio of 1:10, the measured GO/QC ratio determined by TGA was 1:2.20, indicating that only 22% of QC was grafted onto GO nanoflakes. The measured GO/QC ratio plateaus at around the design ratio of 1:5 because of the limited amount of carboxyl groups on GO nanoflakes. The near complete reaction of carboxyl groups on GO with high QC design ratio was confirmed by acid−base titration (see Materials and Methods).

Three clinically significant microbes, specifically *E. coli* (Gram-negative bacterium), *Staphylococcus aureus* (Gram-positive bacterium), and *Candida albicans* (fungus) were chosen as model pathogens to test the antimicrobial activity of GO and GO-QC. Figure 3a shows that GO has poor bacteria- and fungi-killing efficacy of <40%. The QC polymer has excellent antimicrobial activities toward both bacteria and fungi, with respective % kills for these three microbes of 97.5 ± 2.1%, 96.9 ± 2.5%, and 98.8 ± 1.2%. Among the GO-QC nanohybrid series, dramatically higher antimicrobial activities against the three model pathogens compared to those with pristine GO were observed for the two formulations with higher QC contents (Figure 3a). With GO-QC (1:5), the respective % kills for the three microbes are 93.6 ± 4.2%, 97.8 ± 1.8%, and 99.3 ± 0.4%, similar to those of QC ($p > 0.05$, no significant difference). For GO-QC (1:10), the corresponding % kills are 93.7 ± 1.9%, 98.4 ± 1.5%, and 98.2 ± 1.7%, which are similar to those of GO-QC (1:5) ($p > 0.05$, no significant difference). It appears that the antimicrobial activities plateaued beyond

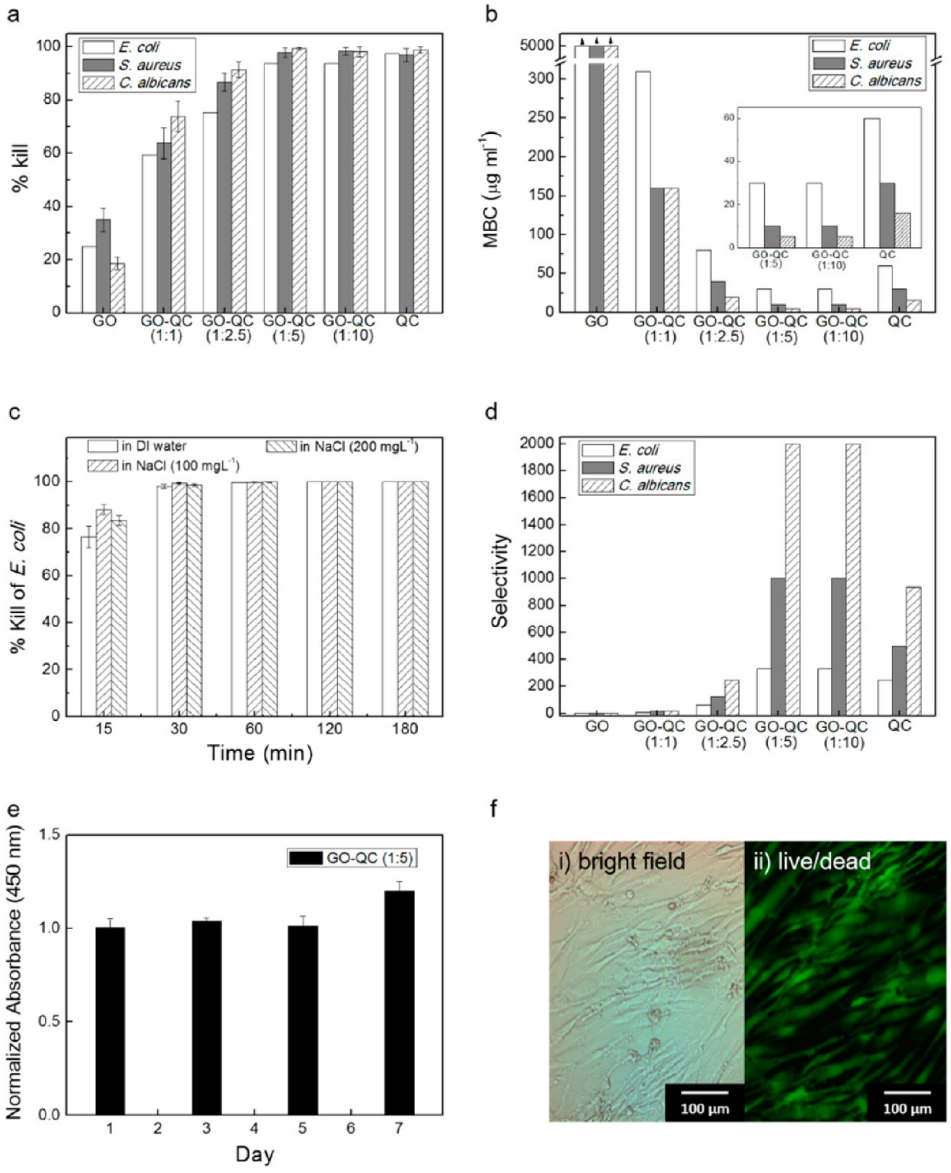

Figure 3. (a) Killing rate of microbes after incubation with GO, QC, and GO-QC series (100 μg mL^{-1}) for 1 h at 10^8 CFU mL^{-1}. (b) Minimum bactericidal concentrations. (c) Antimicrobial activity of GO-QC (1:5) (100 μg mL^{-1}) in DI water and NaCl solution (100 and 200 mg L^{-1}). (d) Selectivity (HC_{50}/MBC). (e) *In vitro* cytotoxicity study of fibroblast cells cultured with 100 μg mL^{-1} GO-QC (1:5). The cell viability was determined by cell counting kit-8 (CCK-8) assay; tissue culture polystyrene was used as the control ($p > 0.05$, no significant difference). (f) Live/dead assay (using calcein-AM and ethidium homodimer-1) of fibroblast cells cultured (i) without and (ii) with 100 μg mL^{-1} GO-QC (1:5) for 7 days.

GO-QC (1:5), corroborating the plateauing of the actual GO/QC ratios inferred from TGA measurements (Table 1). The time dependence of the killing of *E. coli* was also investigated (Supporting Information Figure S5). The % kill by QC and GO-QC reached nearly 100% after 4 h, while the % kill of GO increased more gradually and plateaued beyond 12 h at around 70+% kill.

The MBCs of GO, QC and GO-QC were also determined (Figure 3b and Table 1). The control materials, pristine GO and negatively charged chitosan (nCS), did not show bactericidal activity at concentrations up to 5000 and 2500 μg mL^{-1}, respectively. The QC solution showed good antimicrobial activity with MBCs of 60, 30, and 16 μg mL^{-1} for *E. coli*, *S. aureus*, and *C. albicans*, respectively. The GO-QC (1:5) nanohybrid exhibited improved MBCs in the range of 5−30 μg mL^{-1}, which were lower than those of QC polymer alone. The MBC results of the GO-QC nanohybrids were superior to those of QC polymer solution alone, which is contrary to what is usually achieved with surface immobilization of the polymer.[42] The MBCs plateaued with 1:5 and 1:10 GO-QC, corresponding to the behavior of the % kill. The combination of QC with GO in a nanohybrid enhances the microbicidal potency synergistically.

The time dependence of the killing curve of GO-QC of *E. coli* in DI water and NaCl (100 and 200 mg L^{-1}) was also investigated (Figure 3c). The % kill by GO-QC (1:5)

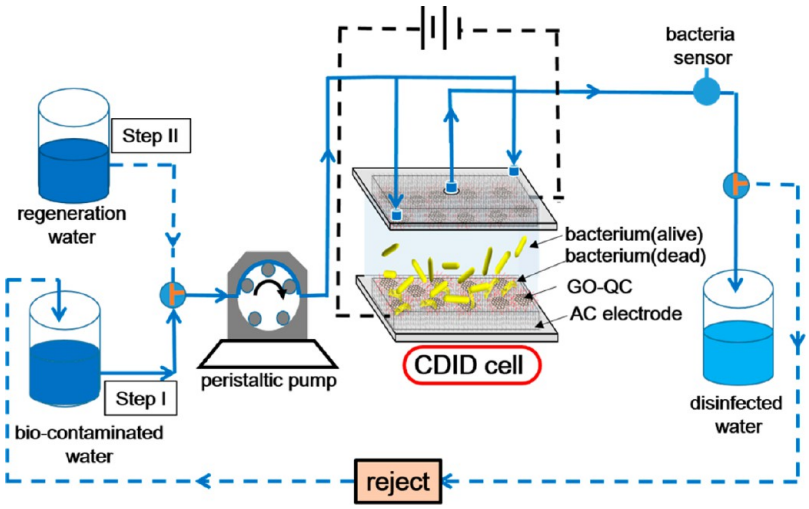

Figure 4. Schematic of the continuous water purification and disinfection (Step I) and regeneration (Step II) of the CDID system.

reached nearly 100% after 1 h in both DI water and NaCl solutions. The presence of salt ions has little effect on the *E. coli* killing, indicating the possible utility of GO-QC for disinfection of brackish water. The antimicrobial activity in the presence of other NaCl concentrations and other salts, including KCl, $MgCl_2$, and $CaCl_2$, is shown in Supporting Information Figure S6.

The GO-QC series generally have 50% hemolysis concentrations (HC_{50}) (Table 1), which are intermediate between those of the two individual components, QC and GO.[43] Both high QC content formulations of GO-QC (1:5 and 1:10) and QC show high HC_{50} values of 10 000 and 15 000 μg mL^{-1}, respectively, much higher than that of pristine GO (1250 μg mL^{-1}). As shown in Figure 3d, the selectivities (defined as HC_{50}/MBC) of GO-QC (1:5) for *S. aureus* and *C. albicans* (1000 and 2000) are significantly improved compared to those of QC alone (500 and 938) and are much improved compared to those of GO. The significant hemolytic activity of GO has been previously reported and is due to the sharp edges of pristine GO which are expected to be harmful to mammalian cells.[44] We have previously shown that chitosan derivatives, such as QC in this report, have low hemolytic activity and low toxicity to mammalian cells.[45] The QC molecules surrounding the GO-QC nanohybrid likely function as a biocompatible protection layer which lowers the frequency of physical damage to mammalian cells by the GO substrate, so that GO-QC shows a much improved HC_{50} compared with pristine GO. We also found GO-QC to have good *in vitro* biocompatibility. Human fibroblast cells (FibroGRO, Millipore) exposed to GO-QC (1:5) (100 μg mL^{-1}) *in vitro* are as viable as on tissue culture polystyrene (TCPS) dish control (Figure 3e, $p > 0.05$, no significant difference). The *in vitro* live/dead test shows many live cells after lengthy exposure to GO-QC (1:5) (Figure 3f).

A schematic diagram of our CDID process for disinfection of bacteria-contaminated water and regeneration of GO-QC/AC electrodes is shown in Figure 4. The biocontaminated solution was pumped into the CDID cell, where a small voltage (2 V) was applied onto the parallel GO-QC/AC electrodes (Step I, Figure 4). As the solution passed through the space between the electrodes, the ions were absorbed onto the electrodes with the opposite potential; bacteria, in this example, *E. coli*, were attracted to the positive electrode because of their negatively charged cell envelopes. On contact with the GO-QC, the *E. coli* were killed. As more suspension passed through the cell, the electrodes became saturated with bacteria. Electrode saturation was detected by the presence of bacteria in the outflow liquid. Before that point, the regeneration process was started and the electrode polarity was turned off, and regeneration water was pumped into the CDID cell to remove the dead bacteria accumulated on the GO-QC/AC electrode surface (Step II, Figure 4). After regeneration, the cell was then switched back to disinfection mode to treat more biocontaminated water.

Figure 5a shows a FESEM of the surface of an AC electrode (the control). We also attempted to use a QC coating on top of the AC electrode to effect disinfection. However, the QC formed a dense continuous layer on the AC electrode and blocked all the pores between the individual AC particles (Figure 5b), making the QC/AC composite insulating and nonfunctional as an electrode (Table 2). GO-QC nanohybrids form a porous surface coating on top of the AC electrode (Figure 5c,d), which allows the solution to reach the AC and current to pass between the electrodes. The GO-QC layer is also somewhat conductive with finite surface resistivity of 4.83 $\pm$ 0.78 MΩ sq^{-1} so that the GO-QC/AC composite can function as an electrode (Table 2). A small amount (10% based on total solid content) of PVDF

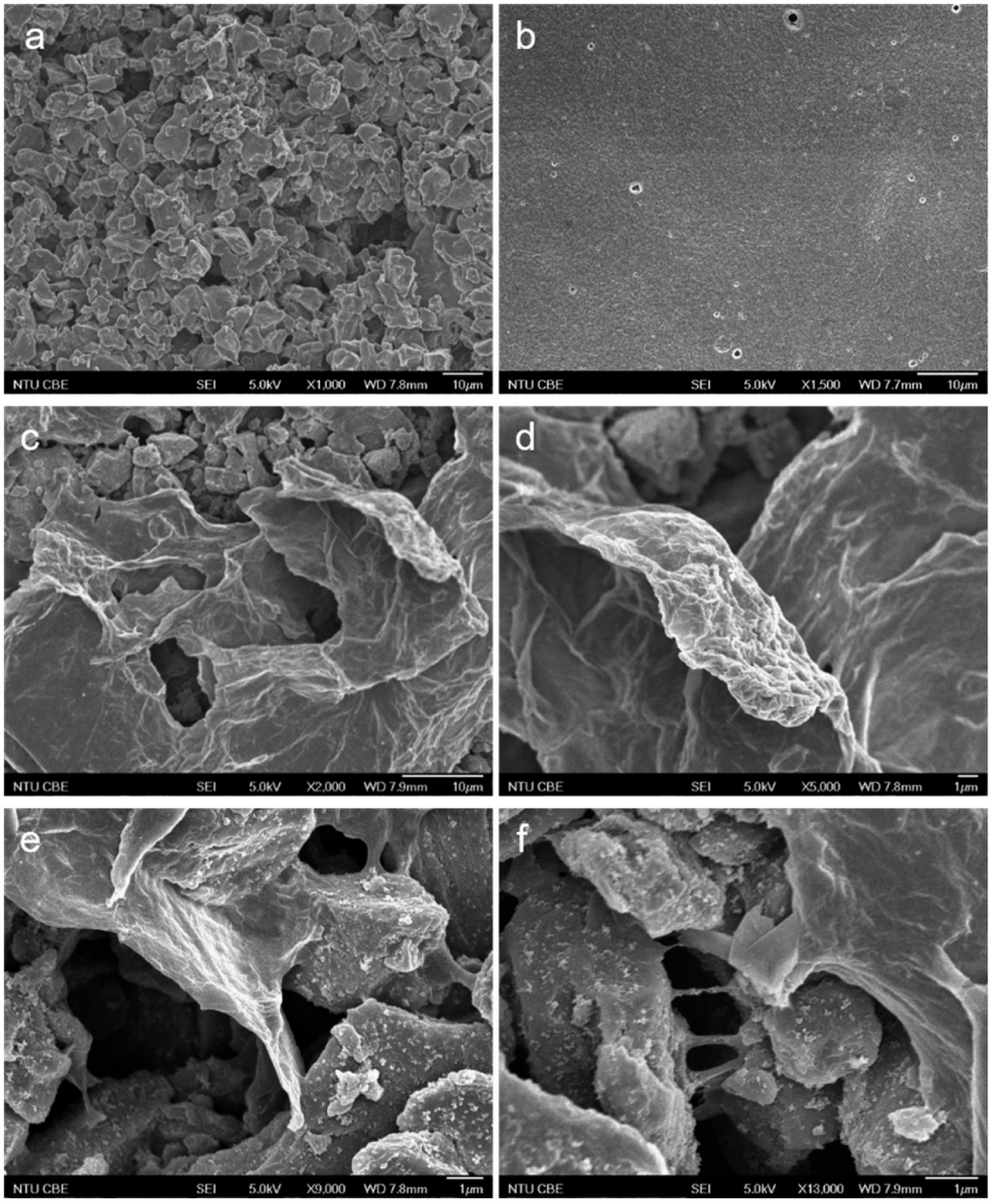

Figure 5. FESEM images for the fabricated disinfecting nanohybrid electrode: (a) pristine AC electrode, (b) QC/AC electrode (c,d) GO-QC/AC electrodes, and (e,f) high-magnification junctions of GO-QC to AC bound by binder (PVDF).

TABLE 2. Resistivity of CDID Electrodes with Different Coating Layer

no.	samples	average (Ω sq^{-1})	standard deviation
1	AC electrode (control)	48	12
2	GO-QC/AC electrode	4,834,500	778,331
3	QC/AC electrode	∞ (nonconductive)	not applicable

binder was mixed into the GO-QC to prevent dislodgement of the nanohybrid from the electrodes into the water, which is highly undesirable. Only a small quantity of binder was needed as the large GO surface enables the GO-QC to be securely bound by PVDF to the AC particles below (Figure 5e,f), and the GO-QC nanohybrid appears to be still freely available for killing bacteria.

The GO-QC/AC electrode was first applied for fast, ultrahigh log reduction of microbes in biocontaminated deionized water. Even with ultrahigh bacteria loading (10^6 CFU mL^{-1}), the GO-QC/AC electrode (Figure 6a) can maintain high log reduction of 6.68 $\pm$ 0.15 (*i.e.*, >99.9999% kill) continuously without any regeneration in the first 20 min; no live *E. coli* was detected at the outlet despite the high loading of bacteria at the inlet (>10^6 CFU mL^{-1}). *E. coli* solution was pumped into the CDID cell at the flow rate of 1 mL min^{-1}, and the voltage was only 2 V. *E. coli* were mostly captured onto the surface of GO-QC/AC

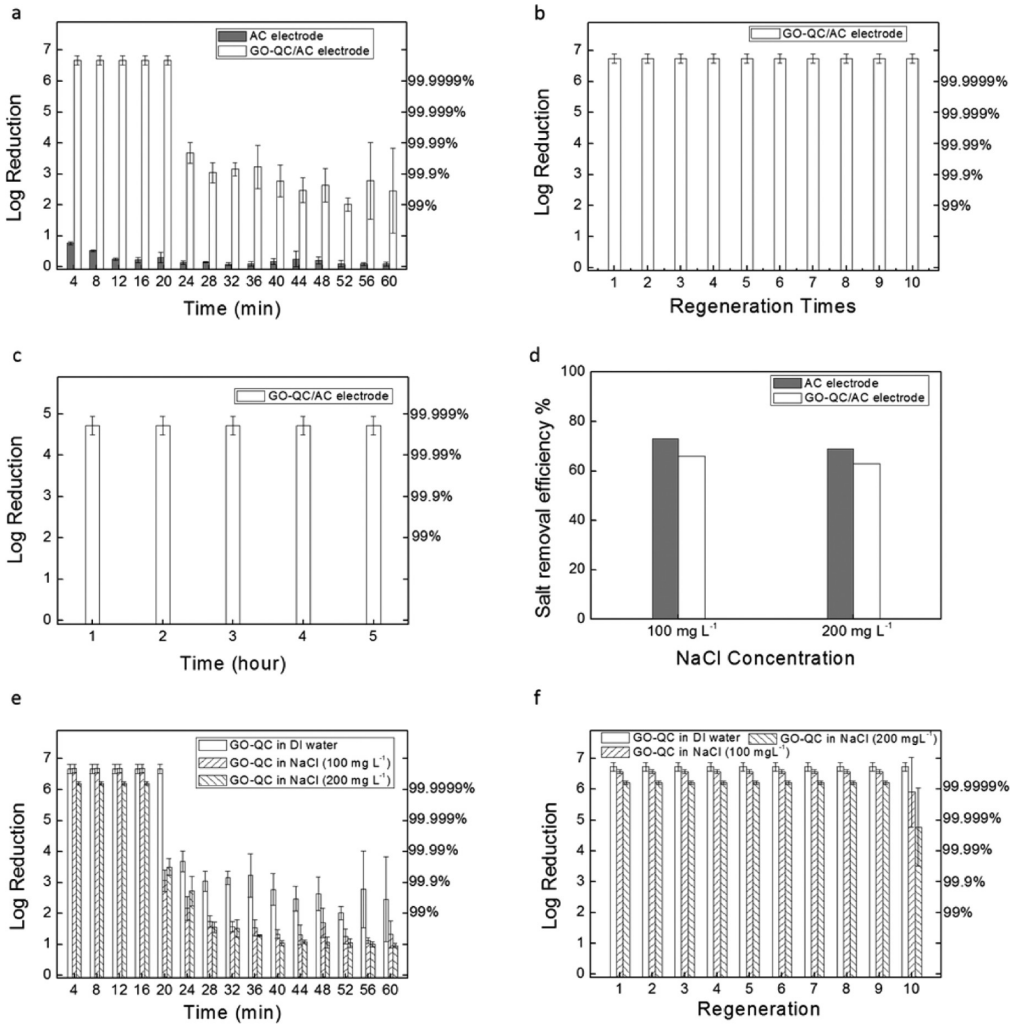

Figure 6. GO-QC/AC CDID cell performance: (a) disinfection performance plot of AC (reference) and GO-QC/AC electrodes and (b) regeneration efficiency of GO-QC/AC electrode. (a,b: *E. coli* concentration is 10^6 CFU mL^{-1}). (c) Disinfection performance plot of GO-QC/AC electrode with lower *E. coli* concentration of 10^4 CFU mL^{-1}. (d) Desalination capacity of AC and GO-QC/AC electrode in NaCl solution (100 and 200 mg L^{-1}) (*E. coli* concentration is 0 CFU mL^{-1}). (e) Disinfection performance plot of CDID with GO-QC/AC electrodes in DI water and NaCl solution (100 and 200 mg L^{-1}). (f) Regeneration efficiency of CDID with GO-QC/AC electrode in DI water and NaCl solution (100 and 200 mg L^{-1}). (e,f: *E. coli* concentration is 10^6 CFU mL^{-1}).

electrode, and clean water flowed out of the CDID cell. After 60 min, the log reduction was still 2.45 ± 1.37, which meant the % kill was 98.5 ± 1.4%. However, with an uncoated AC electrode, the best log reduction of CDID was only 0.76 ± 0.05 (*i.e.*, % removal was 82.8 ± 1.8%) with the same bacteria loading; the bacteria stuck to the AC electrodes were not dead when we cultured them on agar plates. Compared with the typical uncoated AC electrodes used normally for the CDI process, the GO-QC/AC CDID electrodes have an excellent % kill of *E. coli*. The superior disinfection achieved with our CDID process is due to the thin GO-QC layer.

For a typical CDI process to continuously remove ionic species, the electrodes need to be continuously regenerated, and usually, the ion adsorption and electrode regeneration are conducted alternatingly. Recyclability of our GO-QC/AC CDID electrode was also investigated by alternating the voltage from 0 to 2 V at the start of the disinfection step and then switching from 2 to 0 V at the start of the regeneration step. As shown in Figure 6b, the CDID cell maintained its high microbicidal activity with microbe log reduction maintained at around 6.68 ± 0.15 order for over 10 consecutive cycles of alternate disinfection followed by electrode regeneration even with the ultrahigh bacteria loading (10^6 CFU mL^{-1}). Separately, it is noteworthy to mention that no UV peaks characteristic of GO were detected in the exit water after it was flushed into the cell for 1 h (Supporting Information Figure S7), confirming durable attachment of the GO-QC coating to the electrode.

We next evaluated the lifetime of our CDID cell with a moderate bacteria loading (10^4 CFU mL^{-1}) that is relevant to brackish water.[46−48] By running the cell with alternating cycles of 4 min bacteria capture followed by 6 min bacteria desorption, our CDID cell

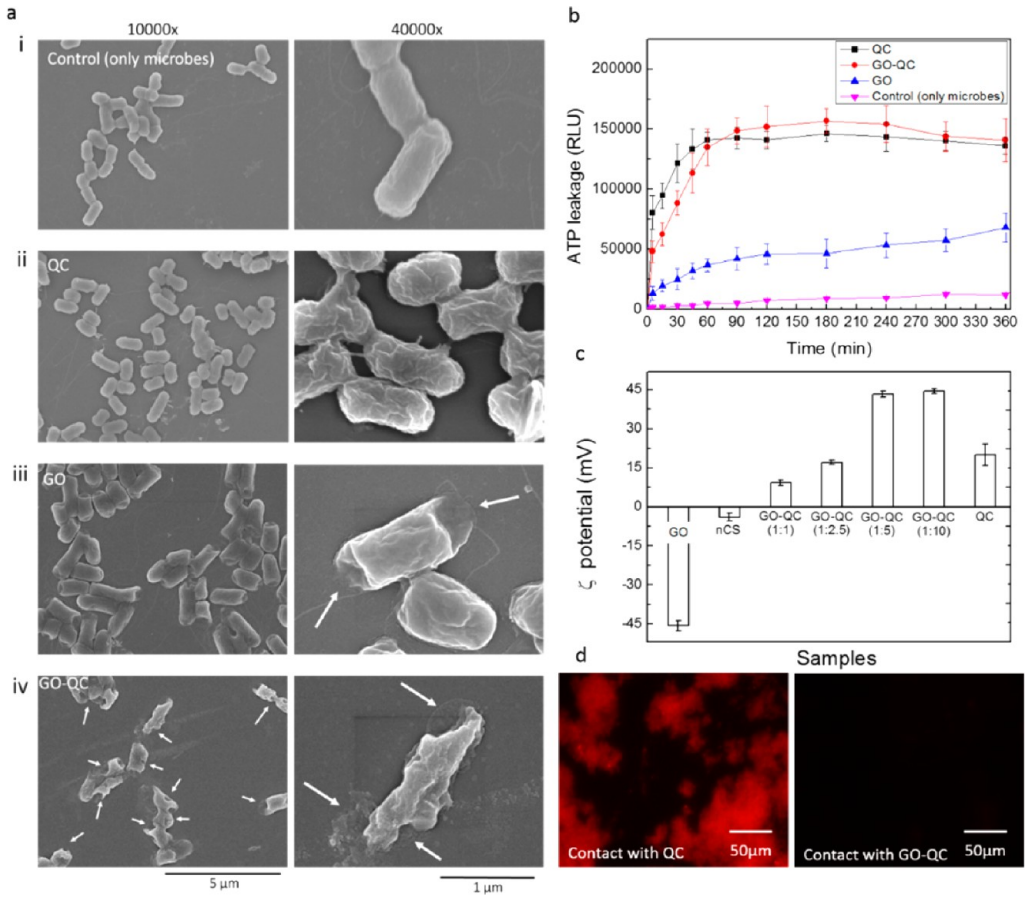

Figure 7. (a) Morphology of *E. coli* (i) untreated control, treated with (ii) QC, (iii) GO, and (iv) GO-QC (1:5) at 100 μg mL^{-1} for 1 h. (b) ATP leakage induced by QC and GO-QC (1:5). (c) ζ-Potential of GO, QC, and GO-QC series. (d) In the fluorescence study, the bacteria (*E. coli*) pellet separated by centrifugation was stained after contact with QC solution but not stained after contact with GO-QC. Both GO-QC and QC molecules were conjugated with a fluorescence dye (Texas Red-X).

can maintain >99.99% kill (*i.e.*, 4 log reduction) of *E. coli* for at least 5 h (Figure 6c).

We also evaluated the salt removal efficiency of our GO-QC/AC CDID cell (Figure 6d). Our GO-QC/AC electrode still retains the initial interconnected porosity of AC with a highly disinfecting GO-QC layer at the top. The laterally large GO-QC nanohybrids form a particulate coating atop the regular porous activated carbon electrode without penetration into the voids to cause malfunctioning of the electrode. Our GO-QC/AC electrode still has a reasonable salt removal efficiency of 66 and 63%, respectively, in noninfected NaCl solution (with 100 and 200 mg L^{-1}) compared to AC CDID cell controls with 73 and 69% efficiency, respectively (Figure 6d). The high salt removal efficiency confirms that our GO-QC/AC electrode could be successfully used for biocontaminated brackish water.

The disinfection of salty water with our CDID cell was also carried out in 100 and 200 mg L^{-1} NaCl solutions with ultrahigh bacteria loading (10^6 CFU mL^{-1}). With Na^+ and Cl^- ions, the time that the cell can achieve 99.9999% *E. coli* killing without any regeneration decreased slightly from 20 to 16 min (Figure 6e). The accumulation of Cl^- ions near the GO-QC layer may reduce its effective cationicity and decrease the killing efficiency. However, with the regeneration cycle included (Figure 6f), the microbicidal activity of the cell was maintained at almost 10 cycles as for deionized water (Figure 6b), as the salts could probably be successfully removed.

We first studied the intrinsic killing mechanism of GO-QC in suspension. FESEM of the morphological changes of *E. coli* cells after contact with QC, GO, and GO-QC (1:5) solution/dispersion (100 μg mL^{-1}) indicates that these materials kill the bacteria by contact-active physical disruption (Figure 7a and Supporting Information Figure S8a). QC-treated *E. coli* cells (Figure 7a(ii)) show wrinkled cell surfaces compared to the smooth surfaces of untreated control cells (Figure 7a(i)). GO-treated *E. coli* cells, on the other hand, are found to have physical defects at the two ends of the cell (arrows in Figure 7a(iii)), which is likely to be produced by the sharp edges of GO nanoflakes. GO-QC (1:5)-treated cells show even more drastic morphological changes compared to those treated with QC or GO: distinct areas of damage (or holes) on the cells can be clearly seen (arrows in Figure 7a(iv)), and the cell envelopes appear severely collapsed,

suggesting physical damage as well as loss of cell contents into the environment. Disruption of the cell membrane can be verified by detecting ATP released into the extracellular environment, stained with a BacTiter-Glo luminescence kit. As shown in Figure 7b, there is significant increase in luminescence after contact with QC and GO-QC, corroborating the FESEM observation of wrinkled cell surfaces that is suggestive of membrane disruption and cell content leakage. Thus, the FESEM study and ATP leakage assay support that the GO-QC nanohybrid effectively disrupts microbial membranes, causing cell death.

We hypothesize that the improved MBC (and selectivity) of the GO-QC nanohybrid compared to either GO or QC is contributed by the higher areal charge density that QC immobilized on GO presents to the cell wall, compared with what exposure to solution QC can produce. The ζ-potential measurements were used to evaluate the charge of the materials (Figure 7c). GO and nCS are negatively charged (-45.8 ± 1.9 and -4.0 ± 1.5 mV, respectively), but the GO-QC nanohybrid is cationic. The ζ-potentials of 1:5 and 1:10 GO-QC (43.4 ± 1.2 and 44.5 ± 1.0 mV, respectively) are even higher than that of QC (20.0 ± 4.2 mV), confirming the hypothesis that the QC molecule is present at higher areal concentration on the GO-QC surface compared to being evenly distributed in QC solution. By comparing the ζ-potentials of the different GO-QC nanohybrid (Figure 7c) to their respective MBCs (Table 1), it is apparent that the MBC improves with increased positive charge, with the best MBC achieved with GO-QC (1:5 and 1:10) possessing the highest positive charge of around +45 mV. The high QC areal concentration on the GO-QC nanohybrid makes electrostatic-induced disruption of the microbe cytoplasmic membrane more effective, thereby decreasing the MBC values to below those of pure QC. Figure 7d shows *via* fluorescence study that there are significant differences in the penetration modes of the two materials (QC *versus* GO-QC) into bacterial cells (*E. coli*). Both GO-QC and QC were conjugated with a fluorescence dye (Texas Red-X), and then the labeled materials were incubated with bacteria. (The conjugation of GO-QC with Texas Red was confirmed by dark-field and fluorescence microscopy; Supporting Information Figure S8b). After 1 h incubation, the bacteria were separated by centrifugation (2000*g*, 10 min) and observed under a fluorescence microscopy. Bacteria incubated with QC-Texas Red were stained red with the fluorescence dye, while the GO-QC-Texas Red did not stain the cells (Figure 7d). We hypothesize that both the free QC in solution and the grafted QC in GO-QC penetrate the cell surface but with different modes. Free QC molecules in solution form are absorbed into the bacterial cell wall and electrostatically bind with the anionic cell envelope so that they cannot be removed by centrifugation. The 2D GO-QC nanohybrids have lateral dimensions comparable to the size of a bacterium and are too large to be absorbed into the cell wall. Other detailed studies of the killing mechanism of the suspended GO-QC are shown in Supporting Information Figures S9 and S10 and related text.

We also studied the killing mechanism of GO-QC when it is part of the composite CDID electrode. Figure 8a,b (indicated by circles and arrows) shows killed *E. coli* covering the surface of the disinfecting GO-QC/AC electrode after the disinfection step. The wrinkled cell surface of dead *E. coli* is apparent (arrows in Figure 8b), which corroborates that GO-QC physically damages the *E. coli* envelope. After the regeneration process, no *E. coli* bacteria can be observed on the electrode surface (Figure 8c,d), which suggests excellent regeneration and recyclability of the GO-QC/AC electrode.

GO-QC exploits the synergistic effects of nanoscale thickness, micron-scale lateral size, and the (partial) conductivity of GO and high charge density due to QC that our grafting procedure produces. Grafting of the GO nanomaterial with cationic QC serves various functions. First, modification of GO with water-soluble cationic QC improves the dispersion of the resulting nanohybrid in an aqueous environment, thus overcoming the aggregation tendencies of GO in solution. Second, the mechanical cytotoxicity of GO nanoflakes to mammalian cells is reduced by grafting with the biocompatible chitosan derivative at their sharp edges. Third, functionalization of GO with cationic quaternized chitosan inverts the charge state of GO from anionic to cationic and endows the GO-QC nanohybrid with net positive charge, so that the anionic bacterial cell envelope will be electrostatically attracted by the cationic GO-QC to result in bacteria cytoplasmic membrane disruption. GO has a large surface area, which enhances its adhesion to the underlying AC electrodes, and it has sufficient conductivity for the GO-QC/AC electrode to function in the CDID process. With GO-QC-coated AC electrodes and a high initial bacteria loading of $>10^6$ CFU mL^{-1}, the % kill of bacteria achievable is >99.9999% and the regeneration potential is at least 10 cycles in both DI water and NaCl solution (100 and 200 mg L^{-1}). The continuous CDID process with our novel GO-QC/AC electrode offers a novel strategy that provides safe, effective, noncontaminating, energy-efficient, and ultrafast contact disinfection of water.

Our single CDID cell employing the GO-QC/AC electrode kills >99.9999% of *E. coli* in DI water in the first 20 min of the disinfection step with ultrahigh bacteria loading (10^6 CFU mL^{-1}); regeneration flushes the dead *E. coli* from the GO-QC/AC electrode, and the >99.9999% killing can be maintained for 10 cycles (~200 min). The ultrahigh *E. coli* concentration in our loading solution (*i.e.*, 1×10^6 to 1×10^7 CFU mL^{-1}) is much higher than that commonly found in brackish water, which typically has a bacteria loading of about 10^4 CFU mL^{-1}.[46−48] We also showed that with a

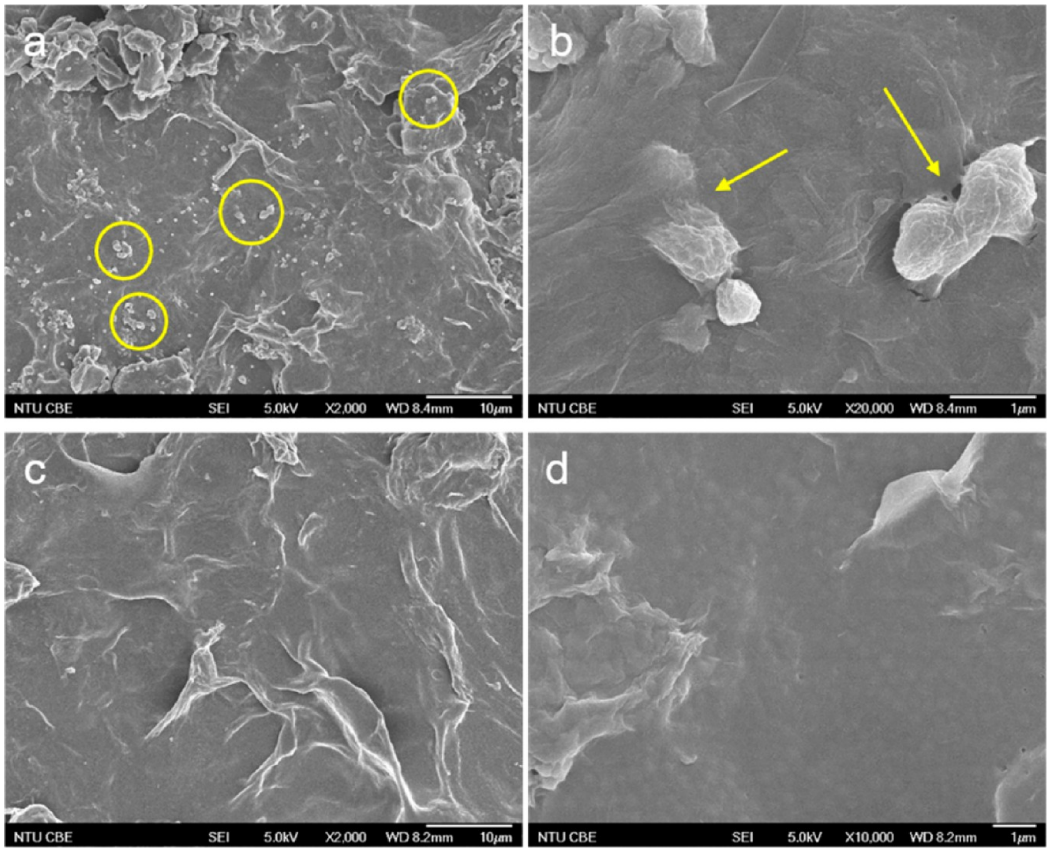

Figure 8. FESEM images of the GO-QC/AC electrode after the disinfection process (a,b) and after the regeneration process (c,d). (The yellow circles and arrows show the dead *E. coli* on the GO-QC/AC electrode and the wrinkled cell surface of dead E. coli in (a) and (b) respectively.)

moderate bacteria loading (10^4 CFU mL^{-1}), the CDID cell can disinfect water continuously for at least 5 h. In our prototype, the GO-QC nanohybrid was simply casted onto the AC layer, but there is great potential for further optimization of the properties of the GO-QC layer, such as the specific surface area, 3D structure, and thickness. Further, the surface area of our cell is about 100 cm^2, and up to 25 or 50 such cells could be connected in stacks or in series. The parallel stacking of hundreds of CDI cells is a common way to increase the processing capacity of salty water in industry;[49,50] this is also a good way to improve the flow rate and killing time of our CDID cell. Considering these factors (cell morphology, geometry, and stacking), the flow rate and durable lifetime of the CDID cell may each potentially be increasable by a factor of 100 or more.[51−54] The optimization of cell parameters has been reported to improve the performance of CDI cells for desalination.[55−57]

There are, at present, numerous technologies that have been developed to disinfect biocontaminated water for drinking, such as ultrafiltration, distillation, and reverse osmosis (RO).[58−60] However, there is still lacking a decontamination process that is continuous, noncontaminating, and yet able to effectively kill and remove bacteria. For example, with RO, chlorine often has to be added upstream of the RO process since bacteria cause biofouling and destroy the membrane, and the current practice of adding chlorine is not ideal for drinking water.[61] Our CDID process can be easily integrated with other such continuous processes.

CONCLUSIONS

A unique disinfecting cationic GO-QC nanohybrid material has been synthesized and explored as part of a novel CDID electrode. The GO-QC nanohybrid forms a thin and porous microbicidal layer on the surface of an AC electrode. The GO-QC/AC electrode can achieve ultrahigh killing (*i.e.*, 99.9999%, 6 log reduction) of 10^6 CFU mL^{-1} *E. coli* in water flowing continuously through the CDID cell. Further, the electrodes can be easily regenerated, with ultrahigh bacteria loading for at least 10 times, even with salt water. With moderate (10^4 CFU mL^{-1}) *E. coli* loading, the CDID can remove and kill at least >99.99% bacteria continuously for at least 5 h. There is no observable GO-QC contamination to the water. Our strategy outperforms all traditional water disinfection processes and has impressive features: no observable residual is left in the purified water, and the GO-QC/AC electrode contact killing process is ultrafast, continuous, energy-efficient (uses only low voltage of 2 V), and easily applicable without expensive equipment.

The GO-QC nanohybrid kills bacteria by contact; it has excellent MBC and selectivity values against representative Gram-negative, Gram-positive, and fungi species, even compared with the individual components (GO or QC alone). The single atomic layer GO with high functionality enables dense surface grafting of the cationic QC and low mass contribution of the GO carrier so that the MBC of this nanohybrid is outstanding. The GO also contributes conductivity to the GO-QC CDID electrode and enables the hybrid to be bound securely by the binder to the AC electrode. This CDID process with the GO-QC nanohybrid-modified electrode that is highly microbicidal, fast-acting, noncontaminating, and energy-efficient has outstanding disinfection application prospects in biomedical, environmental, personal care, and other fields.

MATERIALS AND METHODS

Preparation of Quaternized Chitosan. Quaternized chitosan was synthesized according to a method that we had previously reported.[24] Briefly, a chitosan solution was prepared by dissolving chitosan (1 g, 6.2 mmol monosaccharide) in 1% acetic acid (100 mL). Then, 0.97 g of decanal was added to the chitosan/acetic acid solution, and the mixture was stirred at room temperature for 1 h. The solution pH was then increased to 4.5 by adding NaOH (1 M). Sodium borohydride (0.35 g, 9.3 mmol) was then added into the mixture, and the stirring was continued for another 1.5 h. After that, the pH was further increased to 10 by adding more NaOH (1 M), and then *N*-decyl chitosan precipitated out of solution. The precipitate was filtered out, and the filtride on the filter paper was washed repeatedly with distilled water until the filtrate became neutral. Soxhlet extraction using ethanol and diethyl ether mixture was performed to remove unreacted reagents. In the next step, 1 g of the resulting *N*-decyl chitosan was then added to a mixed solvent of NMP (50 mL) and NaOH solution (1.5 M, 15 mL). After 30 min of stirring at 50 °C, methylation was performed by adding 1.08 g of sodium iodide (7.2 mmol) and 11.2 g of iodomethane (78.7 mmol) to the mixture with stirring continued for another 24 h. After that, the mixture was suction filtered to remove unreacted reagents. The filtrate was dropped into acetone (400 mL), so that the final solid product would precipitate out, and it was then filtered and vacuum-dried at 50 °C.

Determination of Quaternization Degree. The quaternization degree of the chitosan derivative was estimated from elemental analysis and calculated from the relation

$$\text{quaternization degree} = \frac{\frac{C}{N}\,\text{mol\%(chitosan derivative)} - \frac{C}{N}\,\text{mol\%(chitosan)}}{\frac{C}{N}\,\text{mol\%(chitosan)}} \times 100\%$$

Preparation and Characterization of the GO-QC Nanohybrid. Briefly, GO-QC was prepared by a coupling reaction between GO and QC using 1-ethyl-3-(3-(dimethylamino)propyl)carbodiimide hydrochloride (EDC, Sigma) as a coupling reagent together with *N*-hydroxysuccinimide (NHS) illustrated in Figure 1.[62] After reaction, the suspension was centrifuged (20 000*g*, 2 h) to remove the unreacted GO nanoflakes and then filtered with a polyamide membrane (0.2 μm, Sartorius), and the filter cake was continuously washed with deionized water to remove all unreacted reagents. The solid residue was dispersed in water, dialyzed using a cellulose membrane (Sigma, MWCO 14000) for 3 days, and then freeze-dried. The synthesized GO-QC was characterized by FTIR spectroscopy (Nicolet 5700), XPS, AFM, and TGA (Netzsch STA 409). To prepare different sizes of GO-QC (small, medium, and large), pristine GO was first ultrasonicated for 8 h, 3 h, and 15 min, respectively, using a probe sonicator prior to conjugation with QC. To prepare QC conjugated onto polystyrene spheres (PS-QC), polystyrene spheres with carboxylic groups (carboxyl latex, 4%, 500 nm, Life Technologies) were similarly prepared by conjugating QC using EDC/NHS.

Determination of the Content of Carboxyl Groups of GO and GO-QC. The amount of carboxyl groups present in GO and GO-QC was measured by an acid−base titration method.[63] Fifty milligrams of GO or GO-QC was mixed with 10 mL of NaOH solution (0.1 M) under sonication for 30 min and then stirred for 2 days. The suspension was then dialyzed using a dialysis membrane (Sigma, MWCO 14 000) until the pH of the dialysate became neutral. The amount of water in the combined dialysate was reduced by rotary evaporation, and the concentrate was titrated with 0.1 M HCl to pH 7.00. The amount of carboxyl groups was estimated by the amount of NaOH consumed by GO or GO-QC.

For pristine GO, the determined carboxyl groups content was about 5.1 mmol g^{-1}; for 1:5 and 1:10 GO-QC, the content was 0.6 and 0.5 mmol g^{-1}, respectively. The small amount of carboxyl groups left on GO-QC nanohybrids may be masked by the grafted QC molecules, thus preventing further grafting reaction.

Preparation of Negatively Charged Chitosan (nCS). nCS was prepared following a previously reported procedure with minor adjustment.[64] Briefly, chitosan acetate salt was formed by dissolving chitosan in 1% acetic acid. Insoluble particles were removed by centrifugation (4000*g*, 20 min), and the supernatant was lyophilized. One gram of chitosan acetate salt was fully dissolved in 150 mL of deionized water under stirring, and then 0.5 g of succinic anhydride was added within 10 min. The reaction solution was stirred at room temperature for 1 h, and then its solution pH was adjusted to 8−9 with $NaHCO_3$ (0.2 M), with stirring continued overnight. The solution pH was further increased to 10−11 by adding NaOH (1 M). The mixture was dialyzed in deionized water (MWCO 10 000) for 1 week. The nCS product was obtained by freeze-drying. ^{1}H NMR (300 MHz, D_2O) (Supporting Information Figure S11), δ/ppm: 1.95 (s, CH_3), 2.23−2.76 (m, CH_2CH_2), 3.30−3.90 (m, backbone of CS), 4.85 (s, CH).

Preparation of Microbial Cells. *Escherichia coli* (ATCC8739), *Staphylococcus aureus* (ATCC6538), and *Candida albicans* (ATCC10231) were obtained from American Type Culture Collection. All broths and agar media were purchased from Becton Dickinson Company (Franklin Lakes, USA). For bacteria, a single colony was inoculated in Mueller Hinton (MH) broth and cultured at 37 °C overnight, shaking at 200 rpm. Bacteria were harvested at the mid-logarithmic phase by centrifugation (1000*g*, 10 min) and washed with phosphate buffered saline (PBS) solution to remove the residual nutrition. Fungi were inoculated in yeast-malt (YM) broth and cultured at 28 °C for 2 days and then harvested, centrifuged, and washed in the same ways as the bacteria cells.

Antimicrobial Assay for GO and GO-QC Dispersions. Bacteria or fungi cells were centrifuged, and the pellet was resuspended in water and diluted to the desired concentration. 10^8 CFU cells were inoculated into 1 mL GO/GO-QC dispersions and then incubated at 37 °C (28 °C for fungi) under shaking conditions at 200 rpm for the desired time. The cell numbers were determined by the plate colony counting method. One hundred microliters of 10-fold dilutions was pipetted into a 10 cm culture plate and spread with 50 °C MH agar (YM agar for fungi). The plates were cultured in an incubator at 37 °C (28 °C for fungi) overnight for colony formation. The colony number was counted and the percentage kill determined using the equation below. This experiment was performed in triplicate.

$$\%\text{kill} = \frac{\text{cell count of control} - \text{survivor count on sample}}{\text{cell count of control}} \times 100\%$$

Minimum Bactericidal Concentration Determination. The MBC of GO, QC, and GO-QC was determined using a nutrient-free protocol to eliminate the replication of bacteria.[65] A 2-fold

dilution series of 100 μL of antimicrobial reagent solution was made in a 96-well microplate, and then 100 μL of bacterial/fungal suspensions (10^6 CFU mL^{-1}) was added to each well. The microplate was cultured at 37 °C (28 °C for fungi) for 6 h. After incubation, the sample-treated bacterial/fungal suspensions were plated using MH/YM agar. MBC was determined as the lowest concentration for which no bacterium/fungus growth occurred on the nutrition plates. The test was performed twice independently.

Nanohybrid CDID Electrode Fabrication. To fabricate the carbon support layer for cationic disinfecting CDI electrode, a mixture of activated carbon and polyvinylidene fluoride at the ratio of 9:1 (w/w) was dissolved in a proper amount of anhydrous DMF. A uniform carbon slurry was obtained by mixing the mixture using a high-speed planetary mixer at 20 000 rpm for 20 min. The produced slurry was cast onto a graphite foil using a micrometer adjustable applicator with a specified film thickness of 150 μm and was dried at 50 °C for 2 h at atmospheric pressure and then under vacuum at 50 °C overnight to remove the remaining organic solvent. The cationic disinfecting GO-QC thin film was coated onto the carbon layer with the same ratio of PVDF binder, dried at 50 °C for 2 h, and then soaked in double-distilled water to remove the air bubbles. The final thickness of the cationic GO-QC layer after drying was approximately 20 $\pm$ 3 μm, and the mass of the disinfecting material in the carbon electrode was 1.3 mg cm^{-2}. The active electrode area was 10 $\times$ 10 cm^2.

Percent Killing and Log Reduction Calculation of the CDID Process. The *E. coli* was cultured in MHB broth for 6 h at 37 °C in a shaking incubator at 200 rpm and then harvested by centrifugation, and the pellet was resuspended in water and diluted to the desired concentration. One milliliter of 10^8 CFU cells was diluted into 100 mL of DI water. The fresh *E. coli* (10^6–10^7 CFU mL^{-1}) solution (DI water) was prepared as the starting biocontaminated water. The outflow of CDID was collected at an interval of 4 min for determination of cell numbers by the plate colony counting method. Briefly, 100 μL of 10-, 10^2-, and 10^3-fold dilutions was pipetted into 4 in. culture plates and spread with 50 °C LB agar. The plates were incubated at 37 °C overnight for colony formation. The colony number was counted and the percentage kill determined using the equation below. This experiment was performed in triplicate.

$$\%\text{kill} = \frac{\text{cell count of control} - \text{survivor count on sample}}{\text{cell count of control}} \times 100\%$$

$$\log \text{reduction} = \log \frac{\text{cell count of starting colution}}{\text{survivor count in solution at outlet}}$$

Surface Resistivity Measurements. The surface resistivity of AC, GO-QC/AC, and QC/AC electrodes was determined using a four-point probe station (Keithley 2636A). The AC, GO-QC/AC, and QC/AC electrodes were kept in the oven (set at 80 °C) overnight, and the current–voltage curve was measured with driving electrodes sweeping from 0.1 to 0.2 V with 0.01 V steps.

Microbe Morphology Study. The morphology changes of microorganisms induced by QC, GO, and GO-QC were examined with FESEM (JEOL JSM-6701F). Microbe cells were cultured in the presence of QC, GO, and GO-QC at 100 μg mL^{-1} for 1 h. After incubation, the microbes were centrifuged to the tube bottom and collected (1000*g*, 10 min) and were then fixed with 2.5% glutaraldehyde for 4 h and with 1% osmium tetroxide solution for another 4 h at 4 °C. The fixed microbes were then dehydrated in ethanol series solution with graded concentrations from 20 to 100%, each for 15 min, after which the samples were dried under a nitrogen flow. After the samples were vacuum-dried and coated with platinum, they were observed with FESEM for microbe morphology changes.

ATP Leakage Assay. The membrane disruption activity was also characterized with adenosine triphosphate leakage assay. ATP released from the bacterial cells was determined with BacTiter-Glo microbial cell viability assay kit (Promega, USA) and a luminometer (GloMax 20/20, Promega, USA). Briefly, mid-log phase *E. coli* were harvested by centrifugation (1000*g*, 10 min) and washed with PBS three times. The bacterial suspension was diluted to (1–1.5) $\times$ 10^6 CFU mL^{-1} in PBS, and the antimicrobial reagent was added with a concentration of 100 μg mL^{-1}. At desired time points, 50 μL samples were collected, and the released ATP concentration was determined with BacTiter-Glo kit and luminometer.

ζ-Potential Measurement. The charge states of GO, nCS, QC, and GO-QC at the concentration of 100 μg mL^{-1} in water at pH 7 were measured using a ζ-potential analyzer (ZetaPALS, Brookhaven Instruments Corporation, USA). To determine the surface charge of the different microbe species (*E. coli*, *S. aureus*, and *C. albicans*), 1 mL of each microbial species was centrifuged to remove the culture media, washed with water twice, and resuspended in water for measurement with the same ζ-potential analyzer.

Hemolysis Assay. Human erythrocytes were collected by centrifugation (at 1000*g* for 10 min) of 5 mL of fresh blood from a healthy donor (male, age 25). The separated erythrocytes were washed three times with Tris buffer and then diluted to a concentration of 5% (v/v) with Tris buffer. GO and GO-QC solutions (50 μL) with different concentrations were added to a 96-well microplate, and the same volume of erythrocyte suspension was added to each well. Positive and negative control wells received, respectively, 0.1% Triton X-100 in Tris buffer and Tris buffer instead of the GO or GO-QC solutions. The microplate was incubated in a shaking incubator at 37 °C for 1 h at a shaking speed of 150 rpm. After incubation, the contents of the microplate wells were centrifuged (at 1000*g*) for 10 min. After centrifugation, 80 μL of the supernatant from each well was pipetted to the wells of a new microplate, and another 80 μL of Tris buffer was added to the wells to get a final volume of 160 μL. The absorbance at 540 nm was measured with a microplate spectrophotometer (BIO-RAD Benchmark Plus, USA). The percentage of hemolysis was determined from the following equation:

$$\text{hemolysis}\,(\%) = [(A_p - A_b)/(A_t - A_b)] \times 100\%$$

where A_p is the absorbance value for the GO- or GO-QC-containing sample, A_b is the absorbance value for the negative control, and A_t is the absorbance value for the positive control.

***In Vitro* Biocompatibility Study.** Human foreskin fibroblasts (FibroGRO, Millipore) were seeded into the 24-well culture plates at the density of 0.5 $\times$ 10^5 cells cm^{-2}. The culture medium was supplemented with 100 μg mL^{-1} GO-QC (1:5). On specified days, cells were analyzed with the CCK-8 kit (Sigma, USA) by the absorbance at 450 nm to determine the cell viability.[44] Cells in TCPS wells without GO-QC (1:5) were used as the control. The viability of fibroblasts was also examined with the live/dead assay. After specified cell culture time periods, the cells were stained with live/dead kit (Invitrogen, USA) containing 4 mM ethidium homodimer-1 and 2 mM calcein AM in PBS. After 45 min incubation, the live/dead dye was removed by PBS rinsing, and the cell morphology was observed in fluorescence with an inverted optical microscope (Zeiss, Germany).

Conjugation of Texas Red Dye onto QC and GO-QC. Texas Red-X (10 mg mL^{-1}) and succinimidyl ester (Life Technologies) were incubated with a solution of QC or a suspension of GO-QC for 1 h at 25 °C. The excess unreacted dye was removed by dialyzing for 3 days. To confirm the conjugation of QC on to GO-QC, dark-field microscopy and fluorescence microscopy were used to image the GO-QC-dye hybrid. The result in Supporting Information Figure S8b shows that the red fluorescence takes the shape of the GO-QC nanohybrid, indicating the successful conjugation of the dye onto GO-QC.

Optical Microscopy for Visualization of Microbes Attachment. Ten microliter suspensions of GO, QC, GO-QC, and different microbes were pipetted on a glass slide and covered with a coverslip before being viewed under a confocal microscope (Olympus BX51, Germany), and images were taken using the software, analySIS (Olympus, Germany). To assess the viability of the attached bacteria, the bacteria-GO-QC suspension was first incubated with a BacLight bacterial viability kit (L13152, Invitrogen) for 30 min at room temperature and then placed onto glass slides and viewed under a fluorescence microscope.

Conflict of Interest: The authors declare no competing financial interest.

Acknowledgment. This work was funded and supported by a MOE Tier 3 grant (MOE2013-T3-1-002), a NRF POC (NRF2013NRF-POC002-018), NMRC Ministry of Health Industry Alignment Category 2 (NMRC/MOHIAFCAT2/003/2014), NTU iFood Grant, and a SMART grant (BioSym Subaward Agreement No. 13). We thank M. Tan for assistance with the experiments.

Supporting Information Available: The Supporting Information is available free of charge on the ACS Publications website at DOI: 10.1021/acsnano.5b03763.

Detailed synthesis scheme, GPC spectrum, size distribution, XPS analysis, time dependence of antimicrobial activity, antimicrobial activities in the presence of salts, FESEM images, and supporting references (PDF)

Note Added after ASAP Publication: This paper posted ASAP on 9/25/15. Figure 4 was replaced and the revised version was reposted on 9/28/15.

REFERENCES AND NOTES

1. Shannon, M. A.; Bohn, P. W.; Elimelech, M.; Georgiadis, J. G.; Mariñas, B. J.; Mayes, A. M. Science and Technology for Water Purification in the Coming Decades. *Nature* **2008**, *452*, 301–310.
2. Kumar, S.; Ahlawat, W.; Bhanjana, G.; Heydarifard, S.; Nazhad, M. M.; Dilbaghi, N. Nanotechnology-Based Water Treatment Strategies. *J. Nanosci. Nanotechnol.* **2014**, *14*, 1838–1858.
3. Drake, J. 2015 - the Global Risk Outlook. *Offshore Engineer* **2015**, *40*, 1–14.
4. McDonnell, G.; Russell, A. D. Antiseptics and Disinfectants: Activity, Action, and Resistance. *Clin. Microbiol. Rev.* **1999**, *12*, 147–179.
5. Deborde, M.; von Gunten, U. Reactions of Chlorine with Inorganic and Organic Compounds during Water Treatment—Kinetics and Mechanisms: A Critical Review. *Water Res.* **2008**, *42*, 13–51.
6. Kim, Y.-m.; Farrah, S.; Baney, R. H. Structure—Antimicrobial Activity Relationship for Silanols, a New Class of Disinfectants, Compared with Alcohols and Phenols. *Int. J. Antimicrob. Agents* **2007**, *29*, 217–222.
7. Omidbakhsh, N.; Sattar, S. A. Broad-Spectrum Microbicidal Activity, Toxicologic Assessment, and Materials Compatibility of a New Generation of Accelerated Hydrogen Peroxide-Based Environmental Surface Disinfectant. *Am. J. Infect. Control* **2006**, *34*, 251–257.
8. Silvestry-Rodriguez, N.; Bright, K. R.; Slack, D. C.; Uhlmann, D. R.; Gerba, C. P. Silver As a Residual Disinfectant to Prevent Biofilm Formation in Water Distribution Systems. *Appl. Environ. Microb.(AEM)* **2008**, *74*, 1639–1641.
9. Levy, S. B.; Marshall, B. Antibacterial Resistance Worldwide: Causes, Challenges and Responses. *Nat. Med.* **2004**, *10*, S122–S129.
10. Klevens, R. M.; Morrison, M. A.; Nadle, J.; Petit, S.; Gershman, K.; Ray, S.; Harrison, L. H.; Lynfield, R.; Dumyati, G.; Townes, J. M.; et al. Invasive Methicillin-Resistant *Staphylococcus aureus* Infections in the United States. *JAMA, J. Am. Med. Assoc.* **2007**, *298*, 1763–1771.
11. Hancock, R. E. W.; Sahl, H. G. Antimicrobial and Host-Defense Peptides As New Anti-Infective Therapeutic Strategies. *Nat. Biotechnol.* **2006**, *24*, 1551–1557.
12. Radzishevsky, I. S.; Rotem, S.; Bourdetsky, D.; Navon-Venezia, S.; Carmeli, Y.; Mor, A. Improved Antimicrobial Peptides Based on Acyl-Lysine Oligomers. *Nat. Biotechnol.* **2007**, *25*, 657–659.
13. Fox, J. L. Antimicrobial Peptides Stage a Comeback. *Nat. Biotechnol.* **2013**, *31*, 379–382.
14. Eckert, R. Road to Clinical Efficacy: Challenges and Novel Strategies for Antimicrobial Peptide Development. *Future Microbiol.* **2011**, *6*, 635–651.
15. Fischer, D.; Li, Y. X.; Ahlemeyer, B.; Krieglstein, J.; Kissel, T. *In Vitro* Cytotoxicity Testing of Polycations: Influence of Polymer Structure on Cell Viability and Hemolysis. *Biomaterials* **2003**, *24*, 1121–1131.
16. Li, P.; Poon, Y. F.; Li, W. F.; Zhu, H. Y.; Yeap, S. H.; Cao, Y.; Qi, X. B.; Zhou, C. C.; Lamrani, M.; Beuerman, R. W.; et al. A Polycationic Antimicrobial and Biocompatible Hydrogel with Microbe Membrane Suctioning Ability. *Nat. Mater.* **2011**, *10*, 149–156.
17. Li, P.; Zhou, C.; Rayatpisheh, S.; Ye, K.; Poon, Y. F.; Hammond, P. T.; Duan, H.; Chan-Park, M. B. Cationic Peptidopolysaccharides Show Excellent Broad-Spectrum Antimicrobial Activities and High Selectivity. *Adv. Mater.* **2012**, *24*, 4130–4137.
18. Some, S.; Ho, S.-M.; Dua, P.; Hwang, E.; Shin, Y. H.; Yoo, H.; Kang, J.-S.; Lee, D.-K.; Lee, H. Dual Functions of Highly Potent Graphene Derivative-Poly-L-Lysine Composites to Inhibit Bacteria and Support Human Cells. *ACS Nano* **2012**, *6*, 7151–7161.
19. Dong, H.; Huang, J.; Koepsel, R. R.; Ye, P.; Russell, A. J.; Matyjaszewski, K. Recyclable Antibacterial Magnetic Nanoparticles Grafted with Quaternized Poly(2-(dimethylamino)ethyl methacrylate) Brushes. *Biomacromolecules* **2011**, *12*, 1305–1311.
20. Cai, X.; Tan, S. Z.; Lin, M. S.; Xie, A.; Mai, W. J.; Zhang, X. J.; Lin, Z. D.; Wu, T.; Liu, Y. L. Synergistic Antibacterial Brilliant Blue/Reduced Graphene Oxide/Quaternary Phosphonium Salt Composite with Excellent Water Solubility and Specific Targeting Capability. *Langmuir* **2011**, *27*, 7828–7835.
21. Santos, C. M.; Tria, M. C. R.; Vergara, R.; Ahmed, F.; Advincula, R. C.; Rodrigues, D. F. Antimicrobial Graphene Polymer (PVK-GO) Nanocomposite Films. *Chem. Commun.* **2011**, *47*, 8892–8894.
22. Bao, Q.; Zhang, D.; Qi, P. Synthesis and Characterization of Silver Nanoparticle and Graphene Oxide Nanosheet Composites As a Bactericidal Agent for Water Disinfection. *J. Colloid Interface Sci.* **2011**, *360*, 463–470.
23. Liu, L.; Liu, J. C.; Wang, Y. J.; Yan, X. L.; Sun, D. D. Facile Synthesis of Monodispersed Silver Nanoparticles on Graphene Oxide Sheets with Enhanced Antibacterial Activity. *New J. Chem.* **2011**, *35*, 1418–1423.
24. Nederberg, F.; Zhang, Y.; Tan, J. P. K.; Xu, K. J.; Wang, H. Y.; Yang, C.; Gao, S. J.; Guo, X. D.; Fukushima, K.; Li, L. J.; et al. Biodegradable Nanostructures with Selective Lysis of Microbial Membranes. *Nat. Chem.* **2011**, *3*, 409–414.
25. Shen, J. F.; Shi, M.; Li, N.; Yan, B.; Ma, H. W.; Hu, Y. Z.; Ye, M. X. Facile Synthesis and Application of Ag-Chemically Converted Graphene Nanocomposite. *Nano Res.* **2010**, *3*, 339–349.
26. Zhang, D. H.; Liu, X. H.; Wang, X. Green Synthesis of Graphene Oxide Sheets Decorated by Silver Nanoprisms and Their Anti-Bacterial Properties. *J. Inorg. Biochem.* **2011**, *105*, 1181–1186.
27. Al-Jamal, K. T.; Al-Jamal, W. T.; Wang, J. T. W.; Rubio, N.; Buddle, J.; Gathercole, D.; Zloh, M.; Kostarelos, K. Cationic Poly-L-Lysine Dendrimer Complexes Doxorubicin and Delays Tumor Growth *in Vitro* and *in Vivo*. *ACS Nano* **2013**, *7*, 1905–1917.
28. Rai, M.; Yadav, A.; Gade, A. Silver Nanoparticles As a New Generation of Antimicrobials. *Biotechnol. Adv.* **2009**, *27*, 76–83.
29. Oren, Y. Capacitive Deionization (CDI) for Desalination and Water Treatment - Past, Present and Future (a Review). *Desalination* **2008**, *228*, 10–29.
30. Zhang, D.; Yan, T.; Shi, L.; Peng, Z.; Wen, X.; Zhang, J. Enhanced Capacitive Deionization Performance of Graphene/Carbon Nanotube Composites. *J. Mater. Chem.* **2012**, *22*, 14696–14704.
31. Zhang, D.; Wen, X.; Shi, L.; Yan, T.; Zhang, J. Enhanced Capacitive Deionization of Graphene/Mesoporous Carbon Composites. *Nanoscale* **2012**, *4*, 5440–5446.
32. Farmer, J. Method and Apparatus for Capacitive Deionization, Electrochemical Purification, and Regeneration of Electrodes. U.S. Patent US5954937A, May 19, 1995.
33. Oren, Y. Capacitive Deionization (CDI) for Desalination and Water Treatment - Past, Present and Future (a Review). *Desalination* **2008**, *228*, 10–29.
34. Laxman, K.; Myint, M. T. Z.; Al Abri, M.; Sathe, P.; Dobretsov, S.; Dutta, J. Desalination and Disinfection of Inland

Brackish Ground Water in a Capacitive Deionization Cell Using Nanoporous Activated Carbon Cloth Electrodes. *Desalination* **2015**, *362*, 126–132.
35. Hummers, W. S.; Offeman, R. E. Preparation of Graphitic Oxide. *J. Am. Chem. Soc.* **1958**, *80*, 1339–1339.
36. Kovtyukhova, N. I.; Ollivier, P. J.; Martin, B. R.; Mallouk, T. E.; Chizhik, S. A.; Buzaneva, E. V.; Gorchinskiy, A. D. Layer-by-Layer Assembly of Ultrathin Composite Films from Micron-Sized Graphite Oxide Sheets and Polycations. *Chem. Mater.* **1999**, *11*, 771–778.
37. Dreyer, D. R.; Park, S.; Bielawski, C. W.; Ruoff, R. S. The Chemistry of Graphene Oxide. *Chem. Soc. Rev.* **2010**, *39*, 228–240.
38. El-Deen, A. G.; Choi, J. H.; Kim, C. S.; Khalil, K. A.; Almajid, A. A.; Barakat, N. A. M. TiO_2 Nanorod-Intercalated Reduced Graphene Oxide As High Performance Electrode Material for Membrane Capacitive Deionization. *Desalination* **2015**, *361*, 53–64.
39. Jung, I.; Dikin, D.; Park, S.; Cai, W.; Mielke, S. L.; Ruoff, R. S. Effect of Water Vapor on Electrical Properties of Individual Reduced Graphene Oxide Sheets. *J. Phys. Chem. C* **2008**, *112*, 20264–20268.
40. McAllister, M. J.; Li, J.-L.; Adamson, D. H.; Schniepp, H. C.; Abdala, A. A.; Liu, J.; Herrera-Alonso, M.; Milius, D. L.; Car, R.; Prud'homme, R. K.; et al. Single Sheet Functionalized Graphene by Oxidation and Thermal Expansion of Graphite. *Chem. Mater.* **2007**, *19*, 4396–4404.
41. Spinelli, V. A.; Laranjeira, M. C. M.; Fávere, V. T. Preparation and Characterization of Quaternary Chitosan Salt: Adsorption Equilibrium of Chromium(VI) Ion. *React. Funct. Polym.* **2004**, *61*, 347–352.
42. Bagheri, M.; Beyermann, M.; Dathe, M. Immobilization Reduces the Activity of Surface-Bound Cationic Antimicrobial Peptides with No Influence upon the Activity Spectrum. *Antimicrob. Agents Chemother.* **2009**, *53*, 1132–1141.
43. Sovadinova, I.; Palermo, E. F.; Huang, R.; Thoma, L. M.; Kuroda, K. Mechanism of Polymer-Induced Hemolysis: Nanosized Pore Formation and Osmotic Lysis. *Biomacromolecules* **2011**, *12*, 260–268.
44. Liao, K. H.; Lin, Y. S.; Macosko, C. W.; Haynes, C. L. Cytotoxicity of Graphene Oxide and Graphene in Human Erythrocytes and Skin Fibroblasts. *ACS Appl. Mater. Interfaces* **2011**, *3*, 2607–2615.
45. Li, P.; Zhou, C.; Rayatpisheh, S.; Ye, K.; Poon, Y. F.; Hammond, P. T.; Duan, H. W.; Chan-Park, M. B. Cationic Peptidopolysaccharides Show Excellent Broad-Spectrum Antimicrobial Activities and High Selectivity. *Adv. Mater.* **2012**, *24*, 4130–4137.
46. Morales-Morales, H. A.; Vidal, G.; Olszewski, J.; Rock, C. M.; Dasgupta, D.; Oshima, K. H.; Smith, G. B. Optimization of a Reusable Hollow-Fiber Ultrafilter for Simultaneous Concentration of Enteric Bacteria, Protozoa, and Viruses from Water. *Appl. Environ. Microb.(AEM)* **2003**, *69*, 4098–4102.
47. Wang, Y.; Jia, A.; Wu, Y.; Wu, C.; Chen, L. Disinfection of Bore Well Water with Chlorine Dioxide/Sodium Hypochlorite and Hydrodynamic Cavitation. *Environ. Technol.* **2015**, *36*, 479–484.
48. Humphrey, C. P., Jr; O'Driscoll, M. A.; Zarate, M. A. Evaluation of On-Site Wastewater System *Escherichia coli* Contributions to Shallow Groundwater in Coastal North Carolina. *Water Sci. Technol.* **2011**, *63*, 789–795.
49. Park, K.-H.; Kwak, D.-H. Electrosorption and Electrochemical Properties of Activated-Carbon Sheet Electrode for Capacitive Deionization. *J. Electroana. Chem.* **2014**, *732*, 66–73.
50. Ahmad, F.; Khan, S. J.; Jamal, Y.; Kamran, H.; Ahsan, A.; Ahmad, M.; Khan, A. Desalination of Brackish Water Using Capacitive Deionization (CDI) Technology. *Desalin. Water Treat.* **2015**, 1–8.
51. Wang, Y.; Li, Z.; Wang, J.; Li, J.; Lin, Y. Graphene and Graphene Oxide: Biofunctionalization and Applications in Biotechnology. *Trends Biotechnol.* **2011**, *29*, 205–212.
52. Zou, L.; Qiao, Y.; Wu, X.-S.; Ma, C.-X.; Li, X.; Li, C. M. Synergistic Effect of Titanium Dioxide Nanocrystal/Reduced Graphene Oxide Hybrid on Enhancement of Microbial Electrocatalysis. *J. Power Sources* **2015**, *276*, 208–214.
53. Huang, Y.; Dong, X.; Liu, Y.; Li, L.-J.; Chen, P. Graphene-Based Biosensors for Detection of Bacteria and Their Metabolic Activities. *J. Mater. Chem.* **2011**, *21*, 12358–12362.
54. Sui, Z.; Meng, Q.; Zhang, X.; Ma, R.; Cao, B. Green Synthesis of Carbon Nanotube-Graphene Hybrid Aerogels and Their Use As Versatile Agents for Water Purification. *J. Mater. Chem.* **2012**, *22*, 8767–8771.
55. Yin, H.; Zhao, S.; Wan, J.; Tang, H.; Chang, L.; He, L.; Zhao, H.; Gao, Y.; Tang, Z. Three-Dimensional Graphene/Metal Oxide Nanoparticle Hybrids for High-Performance Capacitive Deionization of Saline Water. *Adv. Mater.* **2013**, *25*, 6270–6276.
56. Wang, H.; Zhang, D.; Yan, T.; Wen, X.; Zhang, J.; Shi, L.; Zhong, Q. Three-Dimensional Macroporous Graphene Architectures As High Performance Electrodes for Capacitive Deionization. *J. Mater. Chem. A* **2013**, *1*, 11778–11789.
57. Li, Z.; Song, B.; Wu, Z.; Lin, Z.; Yao, Y.; Moon, K.-S.; Wong, C. P. 3D Porous Graphene with Ultrahigh Surface Area for Microscale Capacitive Deionization. *Nano Energy* **2015**, *11*, 711–718.
58. Wang, Y.; Mao, R.; Wang, Q.; Yang, Z.; Gao, B.; Zhao, Y. Fulvic Acid Removal Performance and Control of Disinfection By-Product Formation Potential in Coagulation-Ultrafiltration Process. *Desalination* **2012**, *302*, 55–64.
59. Ruiz-Aguirre, A.; Polo-López, M. I.; Fernández-Ibáñez, P.; Zaragoza, G. Assessing the Validity of Solar Membrane Distillation for Disinfection of Contaminated Water. *Desalin. Water Treat.* **2015**, *55*, 2792–2799.
60. Wei, X.; Wang, Z.; Chen, J.; Wang, J.; Wang, S. A Novel Method of Surface Modification on Thin-Film-Composite Reverse Osmosis Membrane by Grafting Hydantoin Derivative. *J. Membr. Sci.* **2010**, *346*, 152–162.
61. Blok, A. J.; Chhasatia, R.; Dilag, J.; Ellis, A. V. Surface Initiated Polydopamine Grafted Poly([2-(methacryoyloxy)ethyl]-trimethylammonium chloride) Coatings to Produce Reverse Osmosis Desalination Membranes with Anti-Biofouling Properties. *J. Membr. Sci.* **2014**, *468*, 216–223.
62. Nakajima, N.; Ikada, Y. Mechanism of Amide Formation by Carbodiimide for Bioconjugation in Aqueous-Media. *Bioconjugate Chem.* **1995**, *6*, 123–130.
63. Yang, X. Y.; Zhang, X. Y.; Ma, Y. F.; Huang, Y.; Wang, Y. S.; Chen, Y. S. Superparamagnetic Graphene Oxide-Fe_3O_4 Nanoparticles Hybrid for Controlled Targeted Drug Carriers. *J. Mater. Chem.* **2009**, *19*, 2710–2714.
64. Xu, P.; Bajaj, G.; Shugg, T.; Van Alstine, W. G.; Yeo, Y. Zwitterionic Chitosan Derivatives for pH-Sensitive Stealth Coating. *Biomacromolecules* **2010**, *11*, 2352–2358.
65. Carpenter, A. W.; Worley, B. V.; Slomberg, D. L.; Schoenfisch, M. H. Dual Action Antimicrobials: Nitric Oxide Release from Quaternary Ammonium-Functionalized Silica Nanoparticles. *Biomacromolecules* **2012**, *13*, 3334–3342.